Point contact spectroscopy of Nb₃Sn crystals: Evidence of a CDW gap related to the martensitic transition

R. Escudero *, F. Morales

Instituto de Investigaciones en Materiales, Universidad Nacional Autónoma de México, A. Postal 70-360, México, D.F. 04510, Mexico

A R T I C L E   I N F O

A B S T R A C T

Two Single crystals of Nb₃Sn presenting the martensitic anomaly at different temperature and shape, as observed with specific heat measurements, were used to study structural features in the electronic density of states with point contact spectroscopy. At high temperature below the martensitic anomaly, we observed different spectroscopic characteristics. One sample displaying a well marked specific heat peak, shows a clearly defined structure in the differential conductance that evolves with temperature and may be associated with changes on the density of states due to the opening of a charge density wave gap. Those features are very dependent on the crystallographics characteristics of the single crystal examined.

© 2010 Elsevier Ltd. All rights reserved.

1. Introduction

Nb₃Sn is a well known intermetallic compound with the cubic A15 crystal structure. This intermetallic alloy presents a cubic to tetragonal martensitic transition at about 40–50 K, depending on the crystal studied, and a superconducting transition at around 18 K [1–3]. From the thermodynamic viewpoint, a martensitic is considered to be a first order transition. However, particularly in this compound, controversial results about the thermodynamic order are not completely clarified [4–7]. Quite recently it was established that this transition is a second or weakly first order thermodynamic transition [8]. One aspect related to this behavior is that in many studied Nb₃Sn samples, frequently the martensitic anomaly was observed only as a small feature, which may be related to diverse causes; imperfections in the samples studied, impurities, defects, vacancies, accumulated stress in the crystal structure at the moment of growth process. Those different factors in the specimens may be one of the reasons for the changes in the size and temperature of the anomaly. In a recent paper [8] this anomaly was observed with extraordinarily clarity in some crystals, but was very faint in others.

The aim of this work is to study with point contact spectroscopy (PCS), using some of the same single crystal specimens already reported [8], changes in the electronic density of states when the high temperature anomaly is shown in different size and temperatures [9].

Accordingly, we used two single crystals that present the martensitic anomaly, as observed by specific heat measurements, in different form and temperature. Those crystal were well characterized by X-ray, and present clear structural differences. In Fig. 1 we show the lattice dimensions of one of the crystals, and in Table 1 and Fig. 2 we display the structural characteristics and the specific heat features for the two used specimens. Our PCS results point to differences in the electronic density of states as observed in the differential conductance versus bias voltage of the two studied specimens. Our initial assumption about this behavior is that the martensitic anomaly could be related to a Peierls distortion via dimerization of Nb atoms and nesting at the Fermi surface, which in turn opens a Charge Density Wave (CDW) gap, as was formulated by Gor'kov, Bhatt and McMillan, and Bilbro and McMillan, many years ago [10,11]. In accordance with those experimental results we raise the hypothesis that the specific heat anomaly will be sharper and well formed if no Nb vacancies exist, thus chains are completely formed; so deficiencies in the chains will disrupt the Nb dimerization and produce an imperfect nesting of the Fermi surface giving an ill form of the CDW gap.

2. Experimental details

The study was performed in high quality single crystal samples. Many of the details of the crystal characteristics can be found in Ref. [8]. The crystals were grown by closed-tube vapor transport with iodine vapor as the transport agent over a period of about

---

* Corresponding author. Tel.: +52 55 5622 4625.
  E-mail address: escu@servidor.unam.mx (R. Escudero).
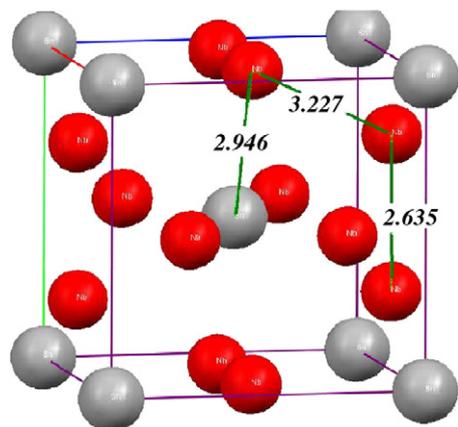
Fig. 1. (Color online) Crystalline structure of Nb_3Sn, NS1 sample and lattice parameters as determined and given in Table 1. Distances are in Å, The grey (big) and red (small) spheres correspond to Sn and Nb respectively, more details are given in Table 1.
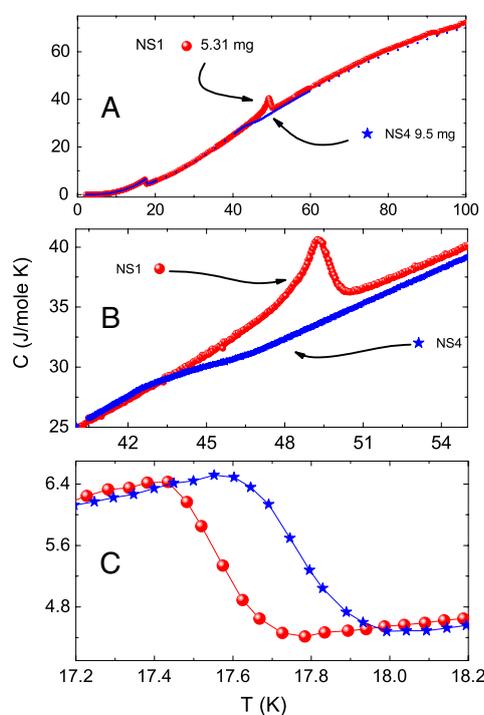
Fig. 2. (Color online) Specific heat around the martensitic and superconducting transitions of two studied samples. Note the different size of the martensitic anomaly that is presented at different temperatures for each specimen; panel B. Panel C shows the superconducting onset differences in temperature, which is small but discernible.

four months. Specific heat capacity measurements were performed from room temperature to 2 K, under a magnetic field below 0.1 Oe. For those measurements we used a thermal relaxation technique with a Quantum Design calorimeter, and a Bachmanns approach for determining the specific heat capacity, as suggested by Lashley, et al. [12]. The crystals were measured and characterized by magnetization versus temperature, resistance versus temperature, and specific heat versus temperature. We present only specific heat measurements which are the most typical results for two different Nb_3Sn samples; named NS1, and NS4.

Point contact spectroscopy junctions were prepared using a fine tip of a gold–tungsten wire of 5 micron diameter. Measurements were performed by contacting the Nb_3Sn samples with the 5 microns wire. The point contact spectra were obtained using the

Table 1
Crystallographic data for two single crystals NS1 and NS4.

Compound	NS1 (5.31 mg)	NS4 (9.5 mg)
Geometric parameters		
Distance		
Nb–Sn (Å)	2.9460 (5)	2.9366 (7)
Nb–Nb (Å)	2.6350 (5)	2.6266 (6)
Nb $\cdots$ Nb (Å)	3.2272 (5)	3.2169 (8)

standard modulation technique consisting of a resistance bridge and lock-in amplifier. More than 20 junctions were measured, and here we will present the most typical results for two different Nb_3Sn samples. PCS measurements show changes in the differential conductance (dI/dV) versus bias voltage (V) at different temperatures from high temperature to about 2 K. Data for sample NS4 were recorded from 80 K to below, whereas for sample NS1 was from 60 K to below. Below the onset of the martensitic anomaly, as specific heat data shows, we observed structure in $dI/dV–V$ in sample NS1, but none in sample NS4. At about 18 K, in both specimens we observed the formation of a single feature related to the superconducting energy gap. The size values, as determined at low temperature, fit well with early tunneling studies in this compound [13–15].

3. Results and discussion

3.1. Crystallographic characterization

An important antecedent of the high quality of the crystals is that others of the same batch were used to perform de Haas van Alphen studies of the Fermi surface. It is important to mention that in order to observe de Hass van Alphen oscillations, the studies require high quality single crystals with a minimum number of imperfections or defects [16].

For the crystallographic characterization we studied two samples by X-ray diffraction, hereafter called NS1 and NS4, with mass of about 5.31 and 9.5 mg, respectively. X-ray characteristics were taken at a temperature of 298(1) K. In addition, we note that no secondary diffraction patterns were observed for possible impurities or diffuse scattering. For each sample, a complete diffraction sphere was collected [17] at the highest available resolution (0.62 Å, $2\theta_{max} = 70°$). A characteristic parameter in a crystal is the high value of the extinction coefficient, which converges to identical values for both samples; so in those crystals we found 0.82(18) for NS1 and 0.8(2) for NS4 [18]. Assuming that applied correction covers mixed primary and secondary extinctions, this result suggests that samples should have similar block sizes and similar concentrations of randomly distributed dislocations [19].

In Table 1 we present some of the characteristics of the two specimens measured. In Fig. 1 is shown the crystal structure of NS1 indicating the distances between atoms. Both samples are characterized by rather short unit cell parameters, $a = 5.2700(9)$ and $a = 5.2531(13)$ Å, for NS1 and NS4, respectively, while the accepted value found in the literature for crystalline Nb_3Sn is $a = 5.29$ Å [20]. Interestingly, NS1 and NS4 have significantly different cell parameters, and, as a consequence, cell volume is reduced by ca 1% in NS4, compared to NS1. Calculated densities present the same 1% drop. However, using diffraction data, a confident interpretation of such a cell contraction in terms of intrinsic vacancies in the alloy cannot be carried out, at least if departures from Nb_3Sn stoichiometry remain small. In contrast, the high resolution of diffraction data allows to accurately determine distances in the crystalline structure. The shortest Nb $\cdots$ Nb separation is reduced from 2.6350(5) Å in NS1 to 2.6266 (6) Å in NS4. In the same

way, Nb···Sn separations in NS1 and NS4 are 2.9460(5) and 2.9366(7) Å, respectively. These differences between the two studied samples may be related with the presence of a high number of defects in the NS4 sample.

3.2. Specific heat measurements

Fig. 2 shows the specific heat of the two studied samples, in the temperature range from 100 K to 2 K (panel A). There, the martensitic transition and the superconducting transition are exhibited. Panel B shows a zoom around the high temperature feature, where a peak is clearly observed for sample NS1, whereas sample NS4 shows only a small and smeared feature. In this same panel it seems that the onset temperatures are quite different. For sample NS1 the onset temperature is about 50 K, whereas for sample NS4 it is around 46.5 K, but difficult to clearly distinguish. In comparison panel C shows the two superconducting transitions, in which the onsets are well distinguished. An important point is worth making: in comparing the onset temperatures in panel B and C, we observed that sample NS1 has a martensitic transition temperature higher than sample NS4, whereas the superconducting transition in the same NS1 sample is lower than that of sample NS4. One possibility of this distinct behavior could be related to a decreasing of the electronic density of states at the Fermi level because of the electron population used to form the CDW gap. This behavior was analyzed and discussed in [8].

3.3. Point contact spectroscopic characteristics

In PCS, one very important parameter is to know the relationship between the electronic mean free path (l) and the point contact diameter (d). For the determination of the point contact region of electron injection, it is assumed in general that the contact is circular; three regimes can be identified and occur for the following conditions: the ballistic regime when $l_e \gg d$, the thermal regime when $l_e, l_{in} \ll d$, and the diffusive regime when $l_e \ll d \ll \sqrt{l_{in}l_e}$, where l_e, and l_{in} are the elastic and inelastic mean free paths, respectively. To extract the correct spectroscopic information from the point contact spectrum, it is necessary to determine the regime of the contact. In the thermal regime there are heating effects in the point contact region; this increases locally the temperature via Joule heating, and the (dI/dV)–V characteristic resembles the resistance temperature dependence of the sample. In this thermal regime the (dI/dV)–V curve does not give information about the superconducting gap. Of course the most appropriate regime to study spectroscopic features on the DOS is the ballistic regime in the first place, and the diffusive limit as a second option. However, experimentally one can find limitations to work in the ballistic regime due to the size of the electronic mean free path. So the diffusive limit is the second option where still we can observe spectroscopic features as the energy gap or phonon influence on DOS. In our experimental PCS junctions we used the formula in [21] for the determination of d,

$$d = \frac{d\rho(T)/dT}{dR_{pc}(T)/dT}. \tag{1}$$

In this equation ρ is the resistivity and R_{pc} is the differential resistance of the point contact at zero bias. We estimate that d is about 100 nm. Nb$_3$Sn is a type II superconductor and has a short electronic mean free path of about 5 nm, this value is lower than d, thus our point contacts will be in the diffusive regime.

Figs. 3 and 4 show the differential conductance as a function of the bias voltage measured at different temperatures from 2 K to 80 and 60 K for two different point contact, Nb$_3$Sn–AuW, with samples NS1 and NS4 respectively.
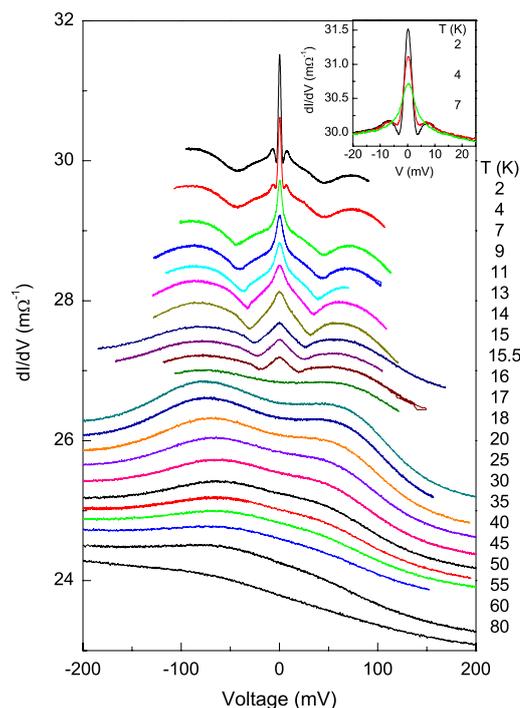
Fig. 3. (Color online) Differential conductance of Nb$_3$Sn(NS1)–Au junction, which presumably has complete Nb chains. Note structure above the superconducting temperature that may be related to the opening of a CDW gap at the martensitic transition, assuming that this is generated by a Peierls distortion, according to Gor'kov, Bhatt–McMillan, Bilbro–McMillan model. For clarity, the curves were displaced relative to the curve measured at 2 K. The inset shows three typical conductance curves of the evolution of the superconducting feature of the PCS junction, at 7, 4, and 2 K.
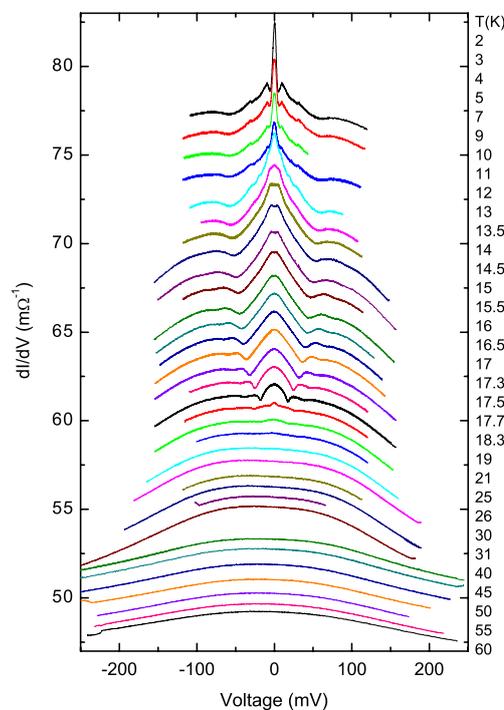
Fig. 4. (Color online) Differential conductance as a function of bias voltage of a Nb$_3$Sn(NS4)–Au point contact junction at various temperatures. Note the absence of structure for above 18 K. The curves were displaced for clarity, relative to the curve measured at 2 K.

At low temperature the curves show the typical feature of the superconducting energy gap around zero bias. The feature
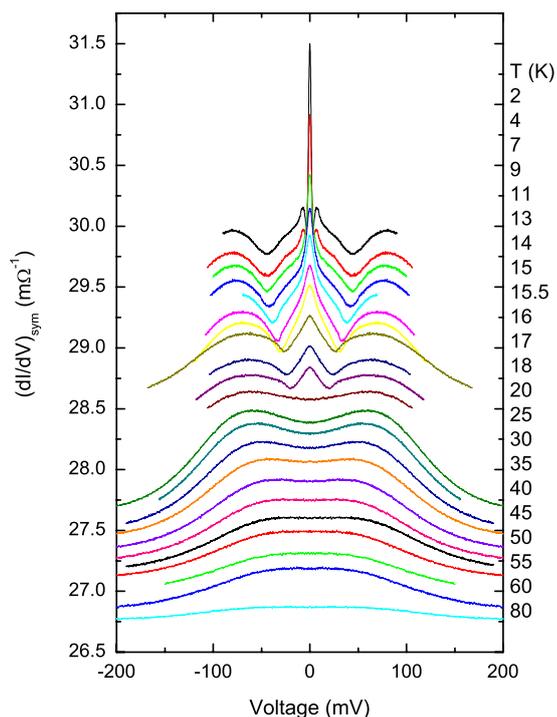
Fig. 5. (Color online) Symmetrized differential conductance as a function of bias voltage of a Nb₃Sn(NS1)–Au point contact from 80 to 2 K. Note the structure below 55 K. The curves were displaced for clarity, related to the curve measured at 2 K.

clearly evolves as the temperature is decreased; at 2 K this feature signature of the energy gap is most notable — see the inset of Fig. 3. The presence of the superconducting energy gap in the point contact spectra gives us the certainty that they are not far of the ballistic regime.

PCS studies in those two samples show different features above the superconducting temperature. Whereas NS1 presents structure in dI/dV–V, which is related in PCS studies to the density of electronic states, in sample NS4 there is no structure at all. A very possible interpretation about this structure may be related to the opening of an energy gap due to the nesting of the Fermi surface by dimerization of Nb chains. In crystal NS1 the chains may be well formed, in comparison to the NS4 crystal. So, NS1 shows a clear CDW gap. Another important observation in sample NS1, on the (dI/dV) characteristics is the structural asymmetry with respect to zero bias. In heterocontacts PCS studies, experts consider that this asymmetry is produced by thermoelectric effects as a consequence of the temperature differences in the contact region and the thermal bath. In order to discard this contribution, the symmetric part of the conductance was determined. The procedure consists in taking the inverse of the symmetric differential resistance, defined as: $(dV/dI)_{sym} = 1/2[dV/dI(V+) + dV/dI(V-)]$ [22].

The symmetrized part, $(dI/dV)_{sym}$ as a function of V, for Fig. 3 is shown in Fig. 5. Two maxima are in these curves; both are at the same positive and negative voltages. Those maxima arise at about 45–50 K, and coincide with the specific heat anomaly onset observed in our measurements. Those maxima evolve and increase with decreasing temperature. At the superconducting transition temperature, one new feature arises; two symmetric minima around zero bias, that also increase as the temperature descend. The physical meaning of this minima, as seen in the differential conductance, is not quite clear, and neither is the type of process that may be involved. However, we believe that this is the effect of the CDW gap and superconducting gap interacting and competing for the same parts of the Fermi surface.
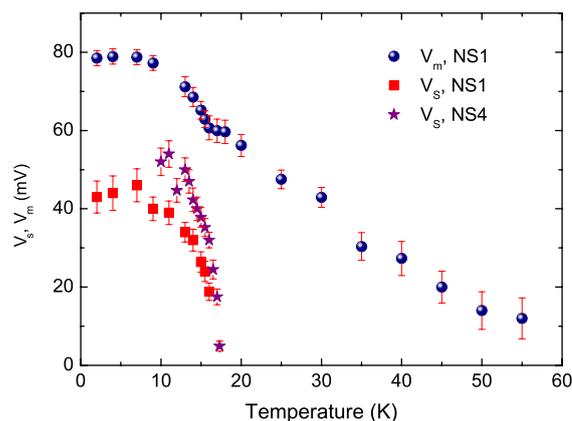
Fig. 6. (Color online) Temperature evolution of the maximum of the differential conductance of the junction of sample NS1. Measured from 55 to 2 K, some interesting features can be seen: (1) the variation of the maximum due to the high temperature anomaly, and (2) the arising of the superconducting temperature at about 18 K.

The temperature variation of the maximum voltage, V_m, defined as the maximum absolute value in $(dI/dV)_{sym}$ is plotted in Fig. 6. The V_m changes with temperature and is shown in this figure. At temperatures from about 65 to 46 K there is no structure, and the $(dI/dV)_{sym}$ curve shows a normal parabolic behavior (see Fig. 5). As soon as the temperature is reduced, the (dI/dV) characteristic is deformed and two maxima arise and increase. Those maxima evolve up to the onset of the superconducting transition temperature. At this onset about 17 K, the $(dI/dV)_{sym}$ looks almost flat. Slightly below this temperature an additional structure arises, which is symmetric around zero bias with two minima at about ±20 mV. The temperature dependence of these minima is plotted in Fig. 6 for NS1 and NS4 samples. The trend of this structure is similar in both samples; however, this structure disappears at 10 K in NS4.

Our speculation about the physical phenomena that originate from the structure observed at high temperature in sample NS1 by the point contact, is that this can be attributed to nesting of parts of the Fermi surface via the formation of a CDW gap. This CDW gap has important consequences related to the strength of the phonon mechanism in A15 compounds.

The Physical phenomena related to nesting of parts of the Fermi surface are in agreement with the theoretical model proposed by Bhatt and Macmillan, and also described by Bilbro and McMillan for A15 intermetallics [11]. This model is based on the Landau theory for phase transformations and on Peierls-like instability, from the physical viewpoint by Gor'kov [10]. In the Peierls instability, the CDW formation is due to nesting of parts of the Fermi surface, via dimerizing chains. In A15 compounds, as in Nb₃Sn, chains are formed by the Nb atoms. Close to the martensitic transition Nb chains are dimerized. The instability decreases the ground state energy of the system, by using a portion of electrons at the Fermi level. The immediate consequence of this phenomenon is the reduction of the superconducting transition, in according with BCS theory. In Fig. 6 we show our observation extracted from the point contact junctions. There, the features observed are related to the modifications to the electronic density of states.

In Fig. 6 we observed the trend of change in V_m and V_s, for the two samples: the voltage V_s associated to the dV/dI minimum related to the size of the superconducting energy gap and the voltage V_m associated to the dI/dV maximum of the CDW gap, of the sample NS1 and NS4. That voltage changes in different forms with temperature for the two samples. Firstly, below 20 K, V_s is

slightly smaller for sample NS1 than for NS4, indicating that the feature related to the superconducting energy gap is small, and decreases below 10 K. Also in that figure, the feature associated to the CDW gap, which starts below 60 K has a clear change at about 17 K; which is the onset of the superconducting state. This feature follows increasing, but now in a small trend, and below 10 K is almost constant. This rate of change, we assume, is due to the interaction between the superconducting state and the nesting of parts of Fermi surface and formation of the CDW gap. We also noted that the superconducting feature of the NS1 sample decreases. At this point it is quite interesting to compare this behavior with Fig. 3 in Bilbro and McMillan's results [11]. In that figure the reduction is in the CDW gap, different to what is occurring in our samples; however this effect can easily be explained considering the strength of the electron phonon in Nb_3Sn. This is given by the ratio; $2\Delta/K_B T_C$, which for the reported superconducting state (similar to our point contact data) is 4.46, [13,15,23,24] whereas for the assumed CDW strengh this ratio is as big as 20–26, indicative of a CDW gap of about $2\Delta = 100$–120 meV.

Thus, the reduction of the martensitic anomaly will increase the electronic population at the Fermi level, therefore increasing the superconducting transition. So as was mentioned before, dimerizing chains reduce the superconducting behavior; thus, defects or Nb deficiencies in Nb_3Sn or in general in A15 superconducting alloys will strengthen superconductivity.

4. Conclusions

Point contact spectra measured into samples NS1 and NS4 present a structure below the martensitic anomaly. The structure is most notable in sample NS1 which presumably has complete Nb chains. We speculated that this structure is the feature related to the opening of a CDW energy gap. In crystal NS4 the structure is ill-defined because the chains are not complete dimerized, due to Nb deficiencies.

References

[1] R. Mailfert, B.W. Batterman, J.J. Hanak, Phys. Lett. 24A (1967) 315.
[2] R. Mailfert, B.W. Batterman, J.J. Hanak, Phys. Status Solidi 32 (1967) K67.
[3] M. Weger, I.B. Goldberg, in: F. Seitz, Turbull (Eds.), Solid State Physics, Vol. 28, Academic Press, New York, 1971, p. 1.
[4] L.J. Vieland, A.W. Wicklund, Solid State Commun. 7 (1969) 37.
[5] C.W. Chu, L.J. Vieland, J. Low Temp. Phys. 17 (1974) 25.
[6] L.J. Vieland, R.W. Cohen, W. Rehwald, Phys. Rev. Lett. 26 (7) (1971) 373.
[7] J. Labbe, J. Friedel, J. Physique (Paris) 27 (1966) 153;
J. Labbe, J. Friedel, J. Physique (Paris) 27 (1966) 708.
[8] R. Escudero, F. Morales, S. Bernes, J. Phys. Condens. Matter 21 (2009) 325701.
[9] W. Weber, L.F. Mattheiss, Phys. Rev. B 25 (1982) 2270.
[10] L.P. Gorkov, Zh. Eksp. Teor. Fiz. Pis'ma Red. 17 (1973) 525 [Sov. Phys. JETP 38 (1974) 830];
L.P. Gorkov, O.N. Dorokhov, J. Low Temp. Phys. 22 (1976) 1; Zh. Eksp. Teor. Fiz. Pis'ma Red. 21 (1975) 656 [JETP Lett. 21 (1975) 310].
[11] R.N. Bhatt, W.L. McMillan, Phys. Rev. B 14 (1976) 1007;
G. Bilbro, W.L. McMillan, Phys. Rev. B 14 (1976) 1887.
[12] J.C. Lashley, M.F. Hundley, A. Migliori, et al., Cryogenics 43 (2003) 369.
[13] D.F. Moore, R.B. Zubeck, J.M. Rowell, M.R. Beasley, Phys. Rev. B 20 (1979) 2721.
[14] J. Geerk, U. Kaufmann, W. Bangert, H. Rietschel, Phys. Rev. B 33 (1986) 1621.
[15] L.Y.L. Shen, Phys. Rev. Lett. 29 (1972) 1082.
[16] A.J. Arko, D.H. Lowndes, F.A. Muller, L.W. Roeland, J. Wolfrat, A.T. van Kessel, H.W. Myron, F.M. Mueller, G.W. Webb, Phys. Rev. Lett. 40 (1978) 1590.
[17] Siemens XSCANS, Version 2.31, Siemens Analytical X-ray Instruments Inc., Madison, WI, USA, 1999.
[18] G.M. Sheldrick, Acta Crystallogr. A 64 (2008) 112.
[19] M. Masimov, Cryst. Res. Technol. 42 (2007) 562.
[20] PDF-19-0875. See also R.G. Maier, Z. Naturforsch. A Phys. Sci. 24 (1969) 1033.
[21] Y.G. Naidyuk, I.K. Yanson, Point-Contact Spectroscopy, in: Solid-State Science, vol. 145, Springer Series, 2005.
[22] A. Nowack, Yu.G. Naidyuk, P.N. Chuvob, I.K. Yanson, A. Menovsky, Z. Phys. B Condens. Matter 88 (1992) 295.
[23] C.P. Poole Jr., H.A. Farach, R.J. Creswick, Superconductivity, Academic Press, Inc., USA, 1995.
[24] J.K. Freericks, Amy Y. Liu, A. Quandt, J. Geerk, Phys. Rev. B 65 (2002) 224510.